

# Supporting Information

Jin et al. 10.1073/pnas.1018859108

## SI Materials and Methods

**Cell Lines, Cell Culture, and Reagents.** Human breast cancer cell lines and the immortalized breast epithelial cells MCF10A were obtained from the American Type Culture Collection through a contract with the National Cancer Institute (IBC45) and through Steve Ethier (Karmanos Cancer Center, Detroit, MI). MCF-7 cells and derivatives were cultured in RPMI medium 1640 supplemented with 10% heat-inactivated FBS, 100 IU/mL penicillin, 100  $\mu$ g/mL streptomycin, and 2 mM L-glutamine. MCF10A cells and derivatives were cultured in DMEM/F-12 medium supplemented with 5% horse serum (Invitrogen), 2 mM glutamine, 100  $\mu$ g/mL streptomycin, 100 IU/mL penicillin, 0.25  $\mu$ g/mL ampicillin B, 100 ng/mL cholera toxin, 20 ng/mL epidermal growth factor (Upstate Biotechnology), 0.5  $\mu$ g/mL hydrocortisone (Calbiochem), and 10  $\mu$ g/mL insulin. The other breast cancer cell lines were grown using media specified by ATCC.

**Soft Agar Colony Formation and Suspension Culture Assays.** Soft agar colony formation assays were performed as described (1). The MCF-7 cell line and its derived cell lines were cultured in DMEM/10% FCS in six-well plates within a 0.35% agar layer. For the MCF10A-Vec and MCF10A-B7 agar colony formation assays, DMEM/Ham's F-12 medium was used, with added components as described for each experiment. The plates were incubated for 10 d (for MCF-7 cells) or 14 d (for MCF10A cells), after which the cultures were inspected and photographed.

**Semiquantitative RT-PCR of EGFR and Its Ligands.** Extraction of total RNA and RT-PCR assay were performed as described previously (2). To compare the PCR products semiquantitatively, samples were collected at intervals of five cycles for 15–40 cycles of PCR to determine the linearity of the PCR amplification; the amplified-Actin cDNA served as an internal control for cDNA quantity and quality. All RNA samples were treated with DNase I to avoid genomic DNA contamination. The sequences of the oligonucleotide primers used for RT-PCR were as follows: EGFR (sense), 5'-GAGAGGAGAACTGCCAGAA-3'; EGFR (antisense), 5'-GTA GCA TTT ATG GAG AGT G-3';  $\beta$ -Actin (sense), 5'-ATG ATA TCG CCG CGC TCG-3';  $\beta$ -Actin (antisense), 5'-CGC TCG GTG AGG ATC TTC A-3'; TGF- $\alpha$  (sense), 5'-CGC CCT GTT CGC TCT GGG TAT-3'; TGF- $\alpha$  (antisense), 5'-AGG AGG TCC GCA TGC TCA CAG; HB-EGF (sense), 5'-AAA AGA AAG AAG AAA GGC AA-3'; HB-EGF (antisense), 5'-CTC CTA TGG TAC CTA AAC AT-3'; Amphiregulin (sense), 5'-AGT CAG AGT TGA ACA GGT AGT TAA G-3'; and Amphiregulin (antisense), 5'-ACT GTA ATA ACA GCA ACA GCT GTG A-3'.

**Measurement of Apoptosis.** Apoptotic cell death was measured by fluorescent microscopic analysis of cell DNA staining patterns with Hoechst 33258 as previously described (1).

**Western Blot Analysis and Antibodies.** Cells were treated and harvested as described. Whole-lysate extracts were prepared as previously described (1). Proteins were resolved by SDS-polyacrylamide (4–12%) gel electrophoresis, transferred to a nitrocellulose membrane, and blotted with the antibodies as indicated. Immunolabeling was visualized by an ECL detection kit from Amersham Biosciences according to the manufacturer's instructions. The antibodies used in this study are as follows: EGFR (BD Biosciences), phospho-active EGFR (BD Biosciences), HOXB7 (Invitrogen), ER $\alpha$  (Santa Cruz Biotechnology), phospho-ER $\alpha$  (ser 118) (Cell Signaling Technology), phospho-p44/42 MAPK (Biosource), TGF- $\alpha$  (Calbiochem), HB-EGF (Calbiochem), Flag (M2) (Stratagene), and p44/42 MAPK (Cell Signaling Technology).

pho-ER $\alpha$  (ser 118) (Cell Signaling Technology), phospho-p44/42 MAPK (Biosource), TGF- $\alpha$  (Calbiochem), HB-EGF (Calbiochem), Flag (M2) (Stratagene), and p44/42 MAPK (Cell Signaling Technology).

**Luciferase Reporter Assay.** Transient transfection was performed with the respective promoter-luciferase constructs. Results were normalized to the level of  $\beta$ -galactosidase activity in the samples. The EGFR promoter reporter plasmids were a kind gift of Alfred C. Johnson (National Institutes of Health, Bethesda, MD). The ERE-tk-LUC plasmid was a generous gift from Elaine Alarid (University of Wisconsin-Madison, Madison, WI).

**Small Interfering RNA Preparation and Transfection.** The siRNA sequences used for targeting human *HOXB7* were 5'-ATA TCC AGC CTC AAG TTC G-3' and 5'-ACT TCT TG TGC GTT TGC TT-3'. The two *HOXB7* siRNA expression plasmids were mixed 1:1 for transfection by use of Effectene (Qiagen).

**Xenograft Analysis.** A total of  $3 \times 10^6$  cells of MCF-7-Vec or MCF-7-B7 were suspended in 100  $\mu$ L PBS/Matrigel (1:1) and injected s.c. into female 3- to 4-wk-old BALB/c nu/nu athymic mice (Sprague-Dawley; Harlan, Madison, WI), which simultaneously received a 60-d slow release pellet containing 0.72 mg of 17 $\beta$ -estradiol and/or 5 mg tamoxifen (Innovative Research of America). Animals were observed once a week. At necropsy, primary tumors, liver, lung, and spleen were evaluated for the presence of macroscopic tumors. Tissue samples of the primary tumor and organs were fixed in 4% paraformaldehyde and stained with H&E to assess histomorphology.

**Chromatin Immunoprecipitation (ChIP) Assay.** ChIP assays were performed essentially as described (3), the IP using anti-Flag M2 antibody or control IgG and amplification of the DNA in the complex using the following primers for the EGFR promoter region: sense, 5'-CAA GGC CAG CCT CTG AT-3'; antisense, 5'-CCC CTT TCC CTT CTT TTG TT-3'. PCR products were analyzed by agarose gel electrophoresis.

**Magnetic Resonance Imaging of Tumor Cell Invasion and Vascular Volume.** Magnetic resonance (MR) experiments characterizing the ability of cells to degrade extracellular matrix (ECM) were performed on a Bruker 400 MR spectrometer as previously described (4).  $^1\text{H}$  MR imaging was performed every 12 h up to 48 h to visualize the geometry of the ECM gel and to detect changes in its integrity due to invasion and degradation.  $^1\text{H}$  images were acquired with a 2-mm slice thickness, a repetition time of 1 s, an echo time of 30 ms, and an in-plane spatial resolution of 0.078 mm. Perfused cells were maintained at a pH of 7.3, 37  $^\circ\text{C}$  temperature, and oxygenation >10%. MCF-7 cells (parental, empty vector, and *HOXB7* overexpressing) were inoculated in the upper left thoracic mammary fat pad of female severe combined immunodeficient mice. A total of  $2 \times 10^6$  cells were inoculated in a volume of 0.05 mL HBSS (Sigma). Mice were imaged 8–10 wk postinoculation. MRI was done on a Bruker 9.4T spectrometer using a home-built solenoid coil. The mice were anesthetized with an i.p. injection of ketamine (25 mg/kg; Phoenix Scientific) and acepromazine (2.5 mg/kg; Aveco, Phoenix Scientific) diluted in saline. The tail vein was catheterized before placing the animal in the spectrometer. Vascular imaging was performed as previously described (5). Briefly, multislice relaxation rate ( $1/T_1$ ) maps were obtained by a saturation recovery method combined with fast T1SNAPSHOT-FLASH im-

aging. An M0 map with a recovery delay of 10 s was acquired. Then, images of four slices (1 mm thick) were obtained for three relaxation delays (100, 500, and 1,000 ms). These  $T_1$  recovery maps were obtained before an i.v. injection of albumin–gadolinium–diethylenetriaminepentaacetate (Gd-DTPA) in saline (dose of 500 mg/kg). Starting 3 min after the injection, imaging was repeated every 3 min over a 21-min period. At the end of the imaging studies, the  $T_1$  of blood was measured. Vascular volume and vascular permeability maps were generated as previously described (6). MR data were analyzed using IDL (Research Systems). Values of vascular volume and permeability-surface area product were computed for every voxel in the tumor. Computer-assisted visualization was performed using Amira 3.1 (TGS). Tumor volumes used in the studies were  $\sim 140$ – $200$  mm<sup>3</sup>. Statistical analysis was performed using a Kruskal–Wallis analysis followed by a comparison for each pair using Student's *t* test. Values of  $P < 0.05$  were considered significant.

**Tumor Samples and Construction of Tissue Microarray.** A total of 127 breast cancer (BC) samples from patients who underwent surgery

at the First Affiliated Hospital of Anhui Medical University (Hefei, Anhui, People's Republic of China) between 2001 and 2002 were used for the IHC analyses. Tissue microarrays were constructed as previously described (7).

**Immunohistochemistry.** Immunohistochemical analysis of HOXB7 and EGFR protein expression was performed on Tissue Micro-Array (TMA) sections (4  $\mu$ m thick) with monoclonal antibodies against HOXB7 (sc-81292; Santa Cruz Biotechnology) and EGFR (sc-03; Santa Cruz Biotechnology) by the peroxidase-conjugated streptavidin complex method (Histostain-SP Kit; Zymed). For HOXB7, the stains were scored as 1 when there were at least 10% tumor cells staining within the tumor and otherwise were scored as 0. For EGFR, the stains were scored as 0 when there was no specific membrane staining within the tumor and positive when there was any staining of tumor cell membrane above background level. The positive cases were further classified into 1+, 2+, and 3+ on the basis of the staining intensity as previously described (8).

1. Zhu T, et al. (2005) Oncogenic transformation of human mammary epithelial cells by autocrine human growth hormone. *Cancer Res* 65:317–324.
2. Mertani HC, et al. (2001) Autocrine human growth hormone (hGH) regulation of human mammary carcinoma cell gene expression. Identification of CHOP as a mediator of hGH-stimulated human mammary carcinoma cell survival. *J Biol Chem* 276:21464–21475.
3. Sharma D, et al. (2005) Release of methyl CpG binding proteins and histone deacetylase 1 from the estrogen receptor alpha (ER) promoter upon reactivation in ER-negative human breast cancer cells. *Mol Endocrinol* 19:1740–1751.
4. Ackerstaff E, Gimi B, Artemov D, Bhujwala ZM (2007) Anti-inflammatory agent indomethacin reduces invasion and alters metabolism in a human breast cancer cell line. *Neoplasia* 9:222–235.
5. Bhujwala ZM, et al. (2003) Reduction of vascular and permeable regions in solid tumors detected by macromolecular contrast magnetic resonance imaging after treatment with antiangiogenic agent TNP-470. *Clin Cancer Res* 9:355–362.
6. Raman V, et al. (2006) Characterizing vascular parameters in hypoxic regions: A combined magnetic resonance and optical imaging study of a human prostate cancer model. *Cancer Res* 66:9929–9936.
7. Wu ZS, et al. (2011) miR-340 inhibition of breast cancer cell migration and invasion through targeting of oncoprotein c-Met. *Cancer*, in press.
8. Shia J, et al. (2005) Epidermal growth factor receptor expression and gene amplification in colorectal carcinoma: An immunohistochemical and chromogenic in situ hybridization study. *Mod Pathol* 18:1350–1356.

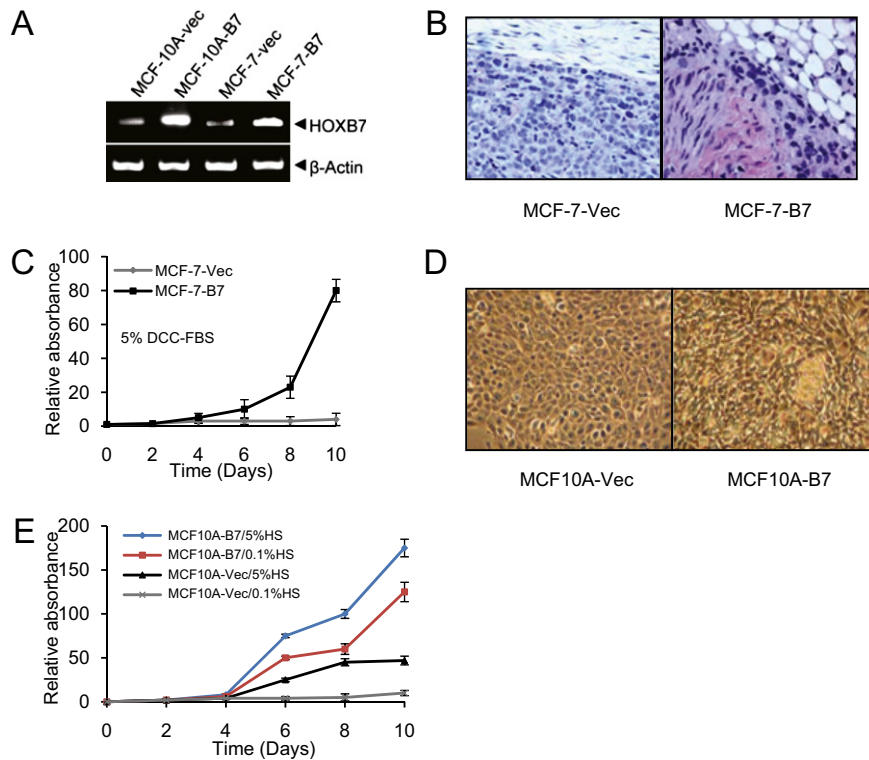


**Fig. S1.** HOXB7 overexpression promotes mammary tumorigenesis. (A) MCF10A cells or MCF-7 cells were stably transfected with either the empty vector (MCF10A-vec, MCF-7-vec) or the vector containing Flag-tagged HOXB7 cDNA (MCF10A-B7, MCF-7-B7). The level of HOXB7 mRNA was determined by RT-PCR. (B) Histologic appearance of the tumors visualized with hematoxylin and eosin staining showing invasion of MCF-7-HOXB7 tumors into the stroma and muscle. (C) Growth curve of MCF-7-Vec and MCF-7-B7 cells grown in an estrogen-deprived condition, in DMEM phenol-free medium containing a 5% Dextran charcoal-stripped serum (DCC-FBS) monolayer culture. (D) Phage-contrast images of MCF10A-Vec and MCF10A-B7 cells cultured to confluence show disorganized growth of HOXB7-overexpressing cells. (E) Monolayer growth curve of MCF10A-Vec or MCF10A-B7 cells in DMEM/F-12 medium. Unlike vector-transfected cells, MCF10A-B7 cells are able to grow even in 0.1% horse serum (HS)-supplemented medium.

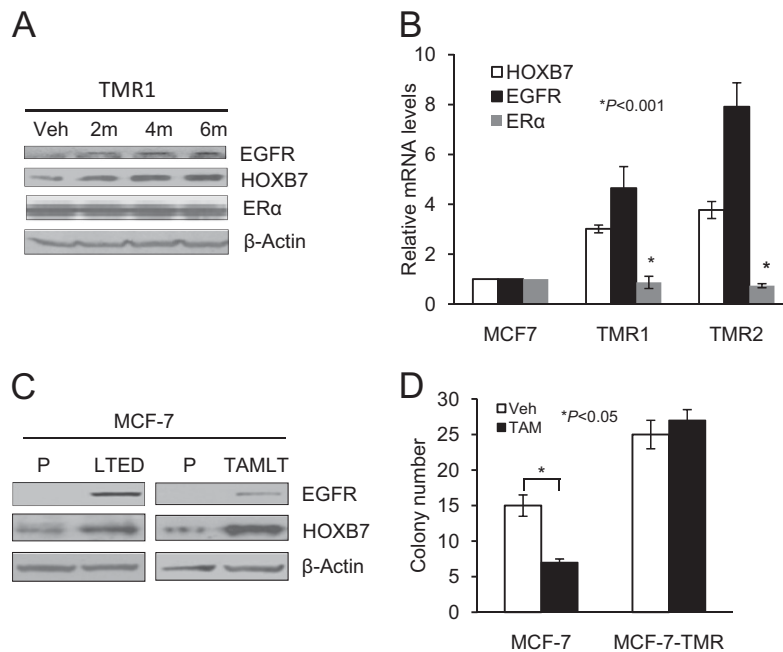


**Fig. S2.** (A) Immunoblot analysis of EGFR, HOXB7, and ERα expression in MCF-7 cells treated with either vehicle for 6 mo or 0.1 μM TAM for 2, 4, and 6 mo. (B) Real-time quantitative PCR analysis of EGFR, HOXB7, and ERα mRNA levels in TMR cells. (C) EGFR and HOXB7 expression in two different anti-estrogen resistance models (MCF-7-LTED and MCF-7-TAMLT). P, Parental cells. (D) Soft agar colony formation by MCF-7 and MCF-7-TMR cells treated with either vehicle or 100 nM tamoxifen. MCF-7-TMR cells do not respond to tamoxifen.



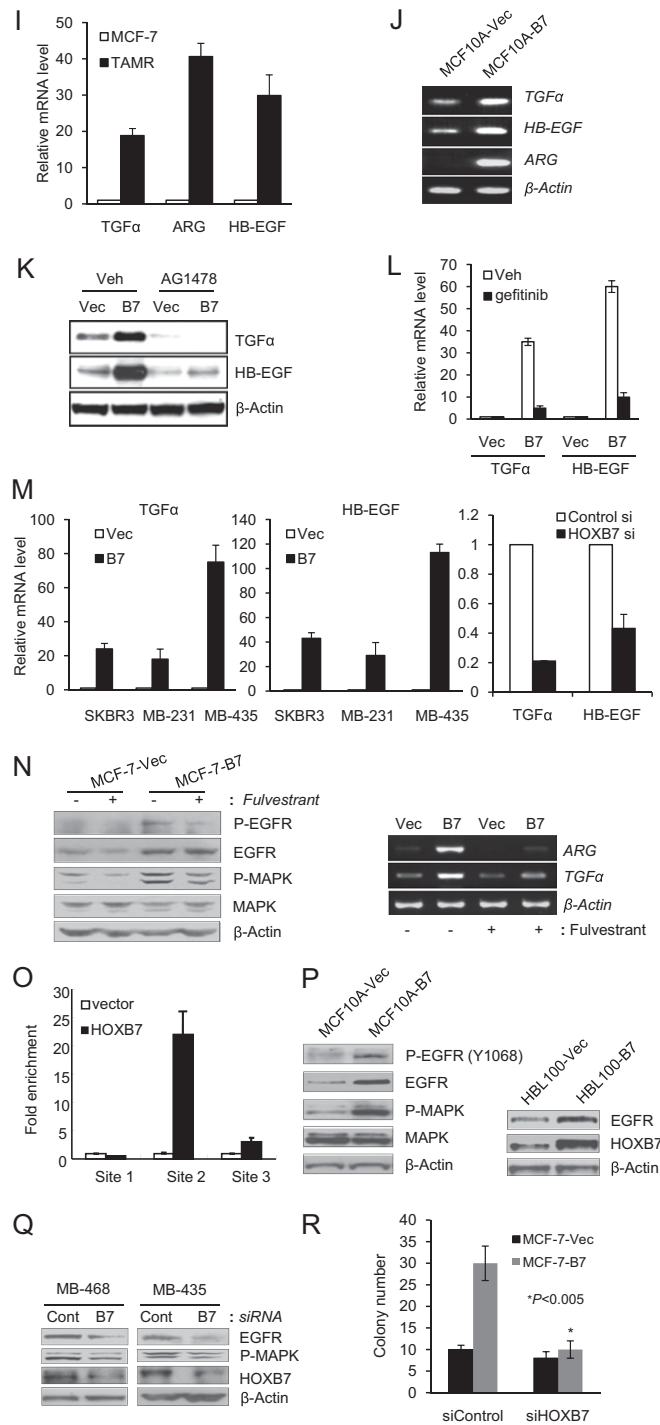


**Fig. S3.** HOXB7 overexpression results in protection from tamoxifen (2  $\mu$ M)-induced apoptosis. (A) Apoptotic cell death was determined by fluorescent microscopic analysis of cell DNA staining patterns with Hoechst 33258 as described in *Materials and Methods*. Bars,  $\pm$ SD in triplicate assays. (B) Cell viability analysis with treatment of 2  $\mu$ M and 5  $\mu$ M TAM by MTT assay in MCF-7-HOXB7 and MCF-7-Vector cells. (C) MCF-7-Vec cells or MCF-7-B7 cells were transfected with ERE-tk-Luc reporter plasmid and  $\beta$ -Gal expression plasmid in the presence of TAM as indicated for 24 h, and reporter activity was measured and normalized by  $\beta$ -Gal activity. (D) Soft agar colony formation by MCF-7-Vec and MCF-7-B7 cells treated with vehicle, 10 nM estrogen, or 1  $\mu$ M TAM in estrogen-deprived medium. (E and F) Tumor growth curve of (E) MCF-7-Vector and (F) MCF-7-HOXB7 cells implanted s.c. in athymic Swiss female mice and treated with either vehicle or TAM (83.3  $\mu$ g/d), in the presence of an exogenous estrogen supplement. (G) Immunoblot analysis of P-EGFR, EGFR, P-MAPK, MAPK, P-ER $\alpha$  (ser118), and ER $\alpha$  in MCF-7-Vec and MCF-7-B7 cells. Cells were incubated in an estrogen-deprived condition for 72 h [DMEM phenol red-free medium containing 5% Dextran charcoal-stripped serum (DCC-FBS)]; cells were then treated with 1  $\mu$ M of TAM at the indicated times. (H) Immunoblot analysis of P-EGFR, EGFR, P-MAPK, MAPK, CyclinD1, and Bcl-2 expression in MCF-7-Vec and MCF-7-B7 cells treated with vehicle, 10 nM estrogen, or 1  $\mu$ M TAM for 24 h in estrogen-deprived medium. (I) Real-time quantitative PCR analysis of TGF- $\alpha$ , Amphiregulin, and HB-EGF mRNA levels in TMR cells. (J) RT-PCR analysis of TGF- $\alpha$ , Amphiregulin, and HB-EGF mRNA levels in MCF10A-HOXB7 cells and vector control cells. (K and L) Immunoblot analysis (K) and real-time quantitative PCR analysis (L) of TGF- $\alpha$  or HB-EGF in MCF10A-B7 cells and the vector control cells treated with 0.1  $\mu$ M AG1478 or 1  $\mu$ M gefitinib or vehicle for 24 h. (M) Real-time quantitative PCR analysis of TGF- $\alpha$ , Amphiregulin, and HB-EGF mRNA levels in HOXB7-SKBR3, MDA-MB-231, and MDA-MB-435 cells and depletion of HOXB7-

Legend continued on following page

MDA-MB-435 cells. (N) Immunoblot analysis of P-EGFR, EGFR, P-MAPK, and MAPK expression in MCF-7-Vec and MCF-7-B7 cells treated with either vehicle or 1  $\mu$ M of fulvestrant for 24 h and RT-PCR analysis of Amphiregulin or TGF- $\alpha$  mRNA expression in MCF-7-Vec and MCF-7-B7 cells treated with either vehicle or 1  $\mu$ M of fulvestrant for 24 h. (O) Real-time quantitative PCR analysis of the putative HOXB7 binding sites in the EGFR promoter region after HOXB7 ChIP assay. (P) Immunoblot analysis of P-EGFR, EGFR, P-MAPK, and MAPK in MCF10A-HOXB7 cells and vector control cells and immunoblot analysis of EGFR and HOXB7 in transient expression of HOXB7 in HBL-100 and vector control cells. (Q) Expression levels of EGFR, P-MAPK, and HOXB7 in MDA-MB-468 and MDA-MB-435 cells transfected with either scrambled sequence siRNA or HOXB7-specific siRNA. (R) Soft agar colony formation by MCF-7-Vec and MCF-7-B7 cells transfected with either scrambled sequence siRNA or HOXB7-specific siRNA in the presence of 1  $\mu$ M TAM.

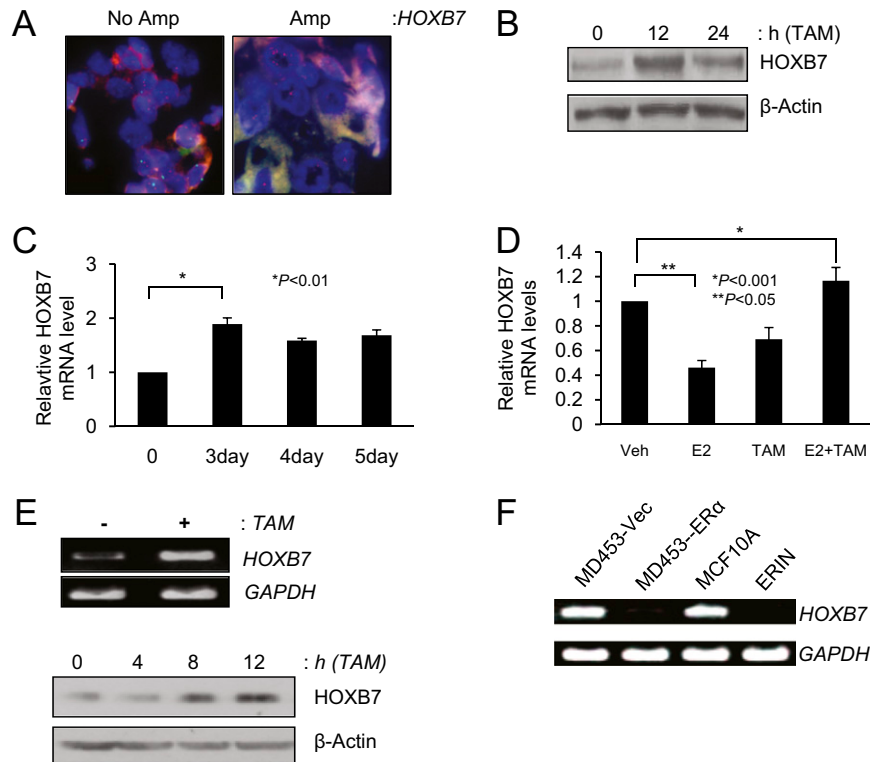


**Fig. 54.** (A) FISH with SpectrumOrange-labeled HOXB7 probe (orange), SpectrumGreen-labeled chromosome 17 centromeric probe (green), and DAPI nuclear stain (blue) in a human tumor sample. Representative images of tumors with (Left) and without (Right) HOXB7 amplification are shown. (B) Immunoblot analysis of HOXB7 expression with treatment of 1  $\mu$ M TAM in MCF-7 cells at the indicated times. (C) Real-time quantitative PCR analysis of HOXB7 in an estrogen-depleted condition for 3–5 d. (D) Real-time quantitative PCR analysis of HOXB7 with 10 nM estrogen, 1  $\mu$ M TAM, or a combination treatment in an estrogen-depleted condition. (E) In the T47D cell line, semiquantitative RT-PCR analysis (Upper) of HOXB7 with 1  $\mu$ M TAM for 24 h and immunoblot analysis at the indicated times (Lower). (F) RT-PCR analysis of HOXB7 expression in MDA-MB-453 cells transiently transfected with ER $\alpha$  and ERIN, ER $\alpha$  stably expressed MCF10A.

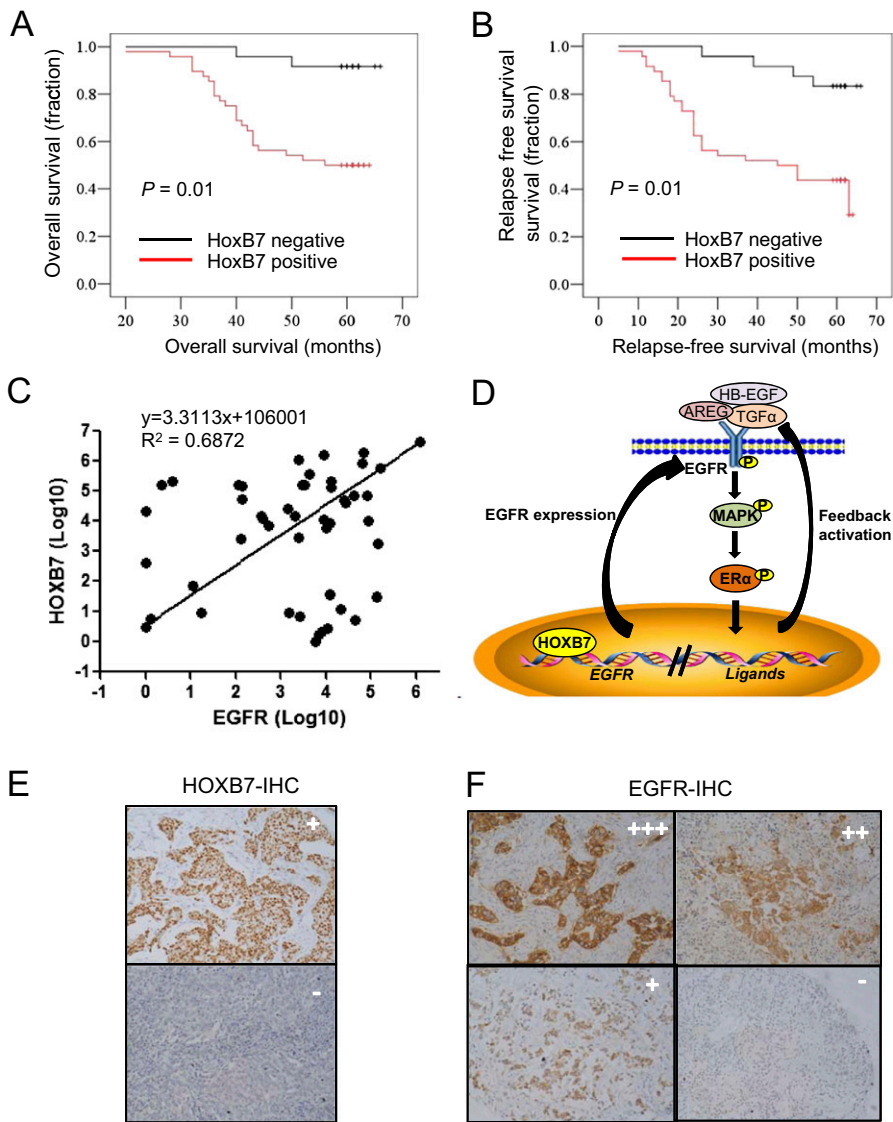


**Fig. S5.** (A and B) Kaplan–Meier plots of (A) overall survival and (B) relapse-free survival analysis of patients with estrogen receptor-positive, node-negative breast cancer who received TAM monotherapy ( $n = 72$ ). (C) Pearson’s correlation between HOXB7 and EGFR mRNA levels in breast cancer cell lines ( $n = 48$ ). (D) Model of HOXB7 regulation of EGFR in tamoxifen resistance. HOXB7 induced by long-term stimulation by tamoxifen is recruited to the EGFR promoter region and enhances EGFR transcriptional activity. Activated EGFR triggers its downstream effectors, MAPK and  $ER\alpha$ , which promote the expression/secretion of EGFR ligands. The positive feedback loop between EGFR and its ligands confers tamoxifen resistance to breast cancer cells. (E and F) Immunohistochemical analysis of HOXB7 and EGFR expression. The intensity of HOXB7 staining was scored as 1 (–, negative) and 2 (+, positive) whereas the intensity of EGFR staining was scored as 1 (–), 2 (+), 3 (++), and 4 (+++).